Trans. Japan Soc. Aero. Space Sci.
Vol. 57, No. 3, pp. 153–159, 2014

Selection of Commercial-Off-the-Shelf Antistatic Coating and Its Applicability for Space-Use Solar Arrays*

By Minoru IWATA,[1)] Akitoshi TAKAHASHI,[1)] Musashi SAKAMOTO,[1)] Mengu CHO[1)] and Ryo MURAGUCHI[2)]

[1)]*Kyushu Institute of Technology, Kitakyushu, Japan*
[2)]*JGC Catalysts and Chemicals Ltd., Kitakyushu, Japan*

(Received May 2nd, 2013)

In recent years, the power generation requirement of spacecrafts has increased in order to load them with many mission devices and to extend their lifetime, hence, high voltages are used. However, such high voltages can cause electrostatic discharges on solar arrays, resulting in damage to the solar arrays. Therefore, we use an antistatic coating, which mitigates the surface charging on solar cells, in order to prevent the discharge. It is considered that an antistatic coating can mitigate surface charging and can prevent discharges on solar cells. The purpose of this research is to develop a coating to mitigate the surface charging applicable to geostationary Earth orbit satellites. We selected a candidate coating with the required surface resistivity and vacuum resistance. Furthermore, we selected a commercial-off-the-shelf antistatic coating after considering the experimental results of charging mitigation performance when simulating the charging condition in space. The candidate agent was coated on a conventional solar array coupon panel, and the charging mitigation performance of the latter was evaluated. We have confirmed a dramatic improvement in charging mitigation performance with this coated conventional solar array coupon.

Key Words: Antistatic Coating, Commercial-Off-the-Shelf, Solar Array, Electrostatic Charging and Discharging

1. Introduction

Since the end of the 1990s, the power level of geostationary Earth orbit (GEO) satellites has increased dramatically. Nowadays, a power level of 10 kW is very common among commercial GEO telecommunication satellites. To sustain such high power generation requires a bus voltage over 100 V to decrease the cable mass and to increase the electrical power transmission efficiency. However, the risk of a power system failure increases with an increase in bus voltage.

Once a substorm occurs, energetic electrons have an impact on spacecrafts, and then the spacecraft chassis potential becomes a highly negative potential of several kV or more with respect to the surrounding plasma potential. Surface insulators on spacecrafts, i.e., coverglasses on solar cells, have a positive potential with respect to that of the spacecraft chassis. Electrostatic discharge easily occurs under the potential condition that is referred to as the inverted potential gradient. Because of the electric-field enhancement at the so-called triple junctions—where vacuum, conductor (interconnector electrode between solar cells), and insulator (coverglass on a solar cell) meet—a discharge is produced under the inverted potential gradient.[1,2)] There are triple junctions on the edge of solar cell components. Therefore, many triple junctions exist, especially on solar array paddles. The discharges on solar arrays would cause short-circuits and would lead to the destruction of the satellite power system, which would result in the loss of all spacecraft functions.

The purpose of this research is to develop a coating applicable to GEO satellite solar arrays, to mitigate surface charging and to prevent discharges on solar arrays. The discharges occur due to anomalous surface charging, which means that parts differ in potential from that of the satellite chassis. By providing an escape path for the stored charges on insulators (coverglasses) that cause the anomalous surface charging, we would avoid discharges on solar arrays. The antistatic coating has the advantage that it would easily prevent discharges at a low cost. For space use, it is, however, necessary to evaluate the charging mitigation performance and durability of the coating in space. In this paper, we evaluated the charging mitigation performance and durability in vacuum of commercial-off-the-shelf (COTS) antistatic coatings.

2. Experiment

2.1. Test sample

2.1.1. Coating

The surface resistivity of antistatic coatings with less than $10^{10}\ \Omega/\square$ is enough to mitigate the surface charging of solar arrays.[3,4)] If the antistatic coatings have a resistivity of $10^{7}\ \Omega/\square$ or more, we could also expect to prevent the leakage of electrical power generated by solar cells. In addition to this, an optical transparency sufficient to generate electrical power on solar cells is required of the antistatic coatings

*Part of this research was presented at the 26th International Symposium on Space Technology and Science, June 4, 2008, Hamamatsu, Japan

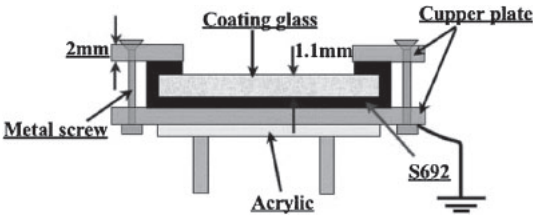

Fig. 1. Test sample structure used in the assessment test.

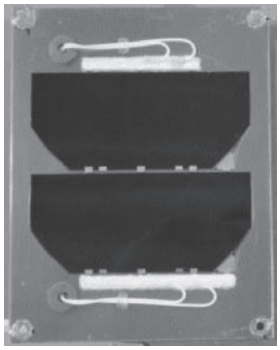

Fig. 2. Solar array coupon used in the validation test.

over the whole solar array paddle. In this study, we use ten kinds of COTS antistatic coating, including a high molecular agent (coating A), three humidity-dependent type agents (coatings B, C, and D), three metal oxide agents (coatings E, F, and G), and three conductive nanoparticle dispersed agents (coatings H, I, and J). The difference between coatings H, I, and J is the concentration of conductive nanoparticles.

For the durability and assessment tests, each antistatic agent is coated on a glass plate by using a dipping method (A, F, and G) or a spray coating method with a portable SPRAYER® unit (B, C, D, and E). Coatings H, I, and J are coated by using a spin-coat method for the durability test and with the SPRAYER® for the assessment test.

2.1.2. Durability test and assessment test with regard to charging mitigation performance

For the durability and assessment tests, we used borosilicate glass (Cosmosvid; Tempax®), which is 90 mm wide, 110 mm long, and 1.1 mm thick. We applied the antistatic coating on the glass and used it as the test sample for these tests. For the assessment test, we attached an electrode to the glass to build an escape path for the surface charge from the glass surface to the electrical ground, as shown in Fig. 1. The electrodes were made of copper and coated with an electrically conductive elastomer adhesive (RTV-S692) to reduce the contact resistance between the copper electrodes and antistatic coatings on the glass. We evaluated the charging mitigation performance by measuring the surface potential change on a 60 mm × 80 mm surface area of the glass in the assessment test.

2.1.3. Validation test using a solar array coupon

Figure 2 shows a solar array coupon used in the validation test for the coatings. The solar cells are triple junction cells (Emcore, ATJ solar cells) and the size of the coupon is 100 mm in width × 130 mm in length. The cover glass is a CMG-100-AR (Qioptiq) with a thickness of 100 µm. The front surface of the cover glass is coated with an antireflective coating (MgF_2). The coupon was made using the same process and materials as a flight solar array paddle based on the baseline design.

2.2. Experimental facility

2.2.1. Durability test under vacuum

The COTS antistatic coatings are developed on the premise that their use in space is excluded. If these coatings are exposed to a high vacuum environment (as well as charged particle radiation, UV, atomic oxygen, etc.), the charging mitigation performance may change. Therefore, we must evaluate the vacuum resistance of COTS antistatic coatings on the properties of charging mitigation.

To evaluate the variation in charging mitigation properties due to vacuum exposure, we store the glass plates coated with COTS antistatic coatings in a vacuum chamber at less than 2×10^{-3} Pa for 48 h. The vacuum storage conditions are determined by the performance and machine time of the vacuum chamber. The vacuum-exposed samples are taken out of the vacuum chamber into the air atmosphere, and then we measure the charging mitigation property immediately after exposure to air. We compare the charging mitigation property of the COTS antistatic coatings before and after vacuum exposure and select highly vacuum-resistant coatings.

In the durability test under vacuum conditions, we evaluate the charging mitigation property by measuring the surface resistivity based on the ASTM-D257 method. A picoammeter (Keithley, Model 6487) and resistivity test fixture (Keithley, Model 8009) were used to measure the surface resistivity of the COTS antistatic coating on glass plates. We apply a voltage of 100 V for a minute and then measure the surface resistivity. Next, we reverse the voltage to 100 V and measure the surface resistivity again. We repeat this voltage reverse 10 times and take an average of the last seven measurement results as the surface resistivity of the COTS antistatic coating.

2.2.2. Assessment test regarding charging mitigation performance

The surface resistivity regarding surface charging potential in space is different from that of ASTM measurement.[5] To simulate charging mitigation behavior in space, we should, therefore, evaluate the charging mitigation performance by measuring the variation of surface potential on an electrified surface. In an assessment test, the coating surface is electrified using electron beam irradiation to simulate the substorm condition in GEO. We measure the surface potential on the coatings over time and evaluate the charging mitigation properties.

The assessment tests are performed in a vacuum chamber that has a cylindrical shape of 600 mm in diameter and 900 mm in length, which is evacuated by a turbo molecular pump to achieve a pressure of 2×10^{-4} Pa. The vacuum chamber is also equipped with an electron gun to simulate

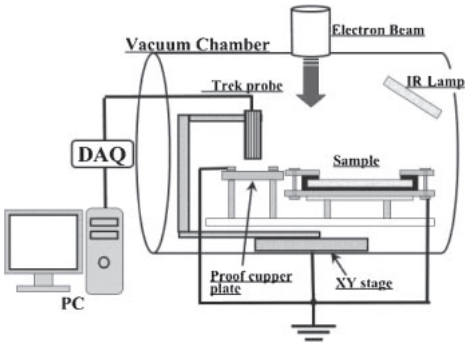

Fig. 3. Experimental system of the Type 1 configuration.

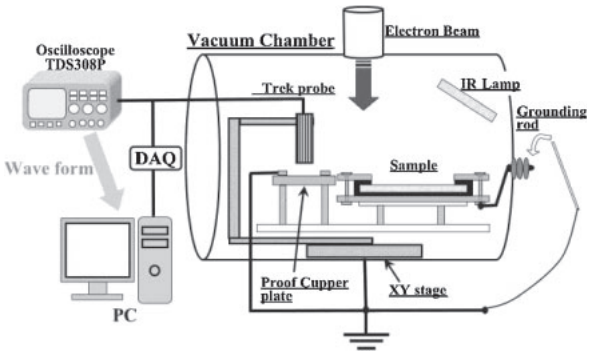

Fig. 4. Experimental system of the Type 2 configuration.

a high-energy substorm electron current in GEO. The two-dimensional distribution of surface potential on the test samples is measured by using a non-contacting surface potential probe (Trek model 341B) attached to an X-Y stage controller unit (Sigma-Koki SGSP26-150 and SGSP26-200). The adsorbed moisture on the sample surface is desorbed due to an infrared lamp heating system inside the vacuum chamber. The baking is carried out for 120 min at 65°C in vacuum at less than 1×10^{-3} Pa before the charging mitigation performance measurements are performed.

First, we perform the assessment test under the Type 1 configuration, in which the test sample electrode is connected to ground. Figure 3 shows the experimental system of the Type 1 configuration. After finishing the baking procedure, the coating surface is electrified with an electron beam having 10 keV of energy and a current of 100 μA for 20 min. The electron beams pass through the aluminum foil to reduce the current density and to uniformly distribute the electron current density. The current density is of the order of $10\,\mu A/m^2$ on the sample surface. The current density is of the same order as that in the substorm condition.[4)] We stop the electron beam irradiation by closing the shutter and measure the two-dimensional distribution of surface potential on the coating surface. Then we irradiate the coating surface for a further 10 min with the electron beam and scan again. These procedures are repeated until the surface potential is saturated. After that, we measure the two-dimensional distribution of the surface potential on the coating surface over time and evaluate the charging mitigation performance of the coatings.

If the charging mitigation is extremely quick and, as a consequence, the coating surfaces are not electrified, we try to perform the assessment test under the Type 2 configuration, in which the test sample electrode is not connected to ground. Figure 4 shows the experimental system of the Type 2 configuration. The procedures saturating the surface potential on the coatings are the same as those in the Type 1 configuration. After the surface potential is saturated, a non-contacting surface potential probe moves to the center of the coating and then the test sample electrode is connected to ground using a grounding rod, as shown in Fig. 4. The variations of surface potential are measured with an oscilloscope (Tektronix: TDS380P, 400 MHz, 2 GS/s).

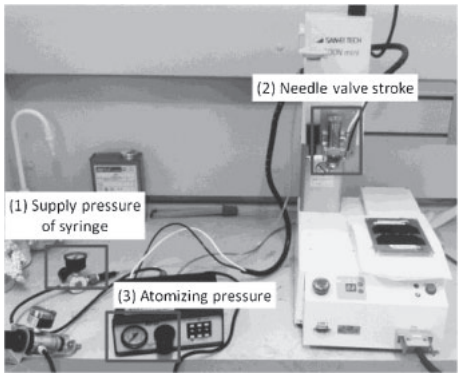

Fig. 5. Dispensing robot.

2.2.3. Validation test

Based on the assessment test results, we select the best coating expected to mitigate the surface charging of the solar array. We apply it on the solar array coupon, as shown in Fig. 2, and then validate the charging mitigation performance on the solar array coupon.

The solar array coupon is coated with a spray method using a dispensing robot (2203N mini, San-Ei Tech Ltd.), as shown in Fig. 5. The robot has the ability to spray an area of up to 200 × 200 mm, due to its X-Y stage. The coating condition is controlled with (1) the supply pressure of a syringe in which the antistatic agent is stored (equivalent to the feed rate of the antistatic agent), (2) the needle valve stroke of the spray nozzle, (3) the air pressure to atomize the antistatic agent fluid into fine droplets, (4) the traverse speed of the X-Y stage, and (5) the distance between the spray nozzle and the sample. In this study, we have selected these parameters, shown in Table 1, and control the coating thickness with the number of coating scans. We coat the entire solar array on a coupon panel five times and then coated the edge of the solar cells five times. After the spraying process, the adhesiveness of the coating is very good. We have rubbed the coated surface with a cloth, but the coating is not been removed from the coupon surface.

In the validation test, the mitigation performance of a solar array coupon panel is evaluated under the Type 1 configuration. The baking is carried out for 120 min at 100°C in vacuum at less than 1×10^{-3} Pa before the charging mitigation performance measurements. After finishing the baking

Table 1. The parameters of the dispensing robot.

Parameter	Set value
(1) Supply pressure of syringe	60 kPa
(2) Needle valve stroke indicator	4
(3) Atomizing pressure	40 kPa
(4) Traverse speed	20 mm/sec
(5) Distance from nozzle	5 cm

Table 2. The number of samples in the durability test.

Coating	Number of samples	
	before vac. exposure	after vac. exposure
A	2	1
B	3	2
C	3	2
D	3	2
E	4	1
F	2	1
G	2	1
H	1	1
I	2	1
J	2	1

procedure, the coating surface is electrified with the electron beam having an energy of 8 to 9.5 keV and a current of 100 μA for 10 min. We stop the electron beam irradiation by closing the shutter and immediately measure the two-dimensional distribution of the surface potential on the coating surface. We evaluated the effectiveness of the coating due to the comparison of charging mitigation on solar array coupons with and without the coating.

3. Results and Discussion

3.1. Durability test under vacuum

The surface resistivity measurement results with the coating before and after vacuum exposure are shown in Fig. 5. Table 2 shows the number of samples in the durability test. In the surface resistivity measurements, the coating surfaces makes contact with test fixture electrodes and suffers some damage. Therefore, the sample is used only once. After vacuum exposure, the surface resistivity of the humidity-dependent agents in coatings B, C, and D significantly increased. The charging mitigation using the coating with a humidity-dependent agent is due to the adsorption of moisture in air. Since the moisture adsorbed on the surface is desorbed in vacuum, the surface resistivity increases after vacuum exposure. For the other seven kinds of coatings, the change in surface resistivity is small after vacuum exposure.

After vacuum exposure, the six kinds of COTS coatings have an electrical conductivity between the upper and lower limits of conductivity. We decided to perform an assessment test for six kinds of COTS antistatic agents. We aim at the electrical conductivity after the vacuum durability test and

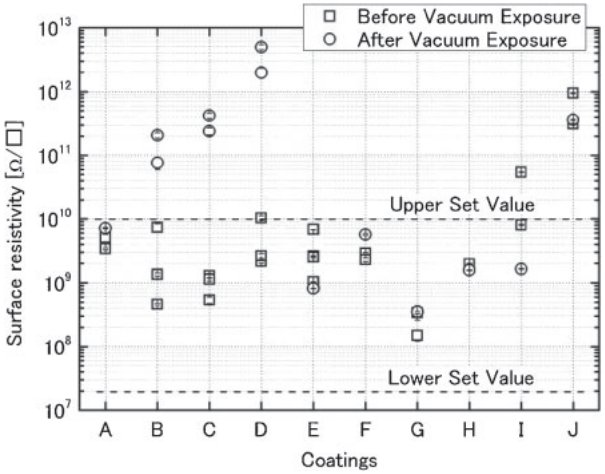

Fig. 6. Durability test results on various COTS antistatic coatings.

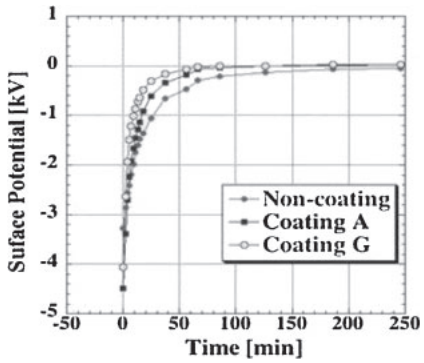

Fig. 7. Assessment test for non-coated and Coatings A and G.

determine the priority for the coatings. We determine the first priority coating to have an electrical conductivity away from the upper and lower limit in Fig. 6. From Fig. 6, the first priority coating is Coating G. Since the electrical conductivities of Coatings E, H, and I are located near the upper limit, the second, third, and fourth priority are Coatings E, H, and I, respectively. There is little priority difference between Coatings E, H, and I. Since the electrical conductivities of Coatings A and F are observed to be very close to the upper limit, the fifth and sixth priorities are the Coatings A and F, respectively. There is also little priority difference between coatings A and F. Therefore, the priority of the coatings was G, E, H, I, A, and F.

3.2. Assessment test

The charging mitigation performance of Coatings A and G was measured with the Type 1 experimental system. Since the charging mitigations of Coatings E, F, H, and I were extremely quick, the surface potentials were measured with the Type 2 experimental system. The surface potential change at the center of the sample are shown in Figs. 7 to 11. In Fig. 7, the surface potential change of a non-coated sample, borosilicate glass, is also shown. As shown in Fig. 7, the charging mitigation of coatings A and G were faster than that of the non-coated sample.

The charging mitigation performance of Coatings E, F, H and I was measured with the Type 2 experimental system.

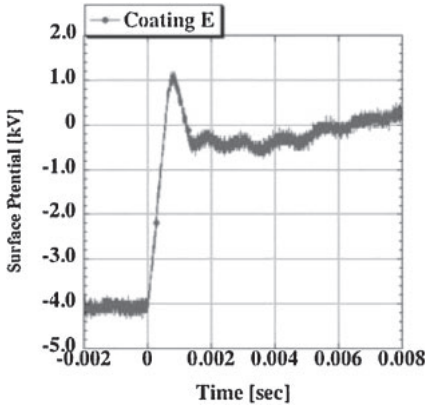

Fig. 8. Assessment test for coating E.

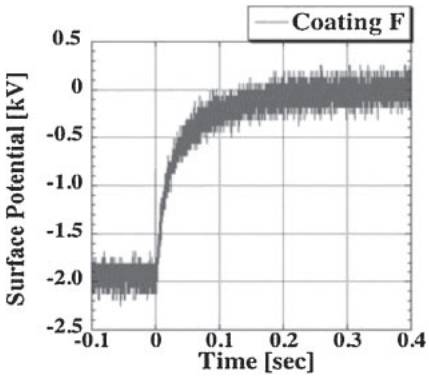

Fig. 9. Assessment test for coating F.

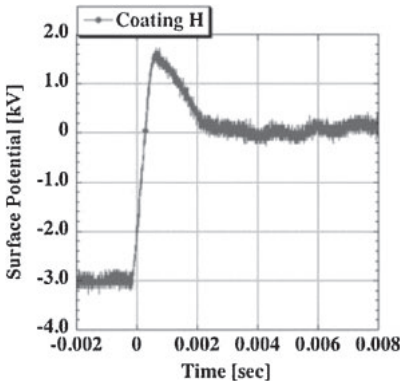

Fig. 10. Assessment test for coating H.

As shown in Fig. 9, the charging mitigation time of Coating F until the surface potential becomes 0 V is about 0.3 sec. On the other hand, the charging mitigation time of Coating E, H, and I until the surface potential becomes 0 V is less than 1.0 msec, as shown in Figs. 8, 10, and 11. The charging mitigation performance of Coatings E, H, and I is superior to that of Coatings A and G. However, we cannot control the surface resistivity of Coating E to the desired value. On the other hand, we obtained a different surface resistivity for Coatings H and I due to the dispersion of the different concentrations of conductive nanoparticles in common matrix materials. Coatings H and I have the advantage that the surface resistivity could be controlled to the desired value. Therefore, Coating H was selected for the validation test.

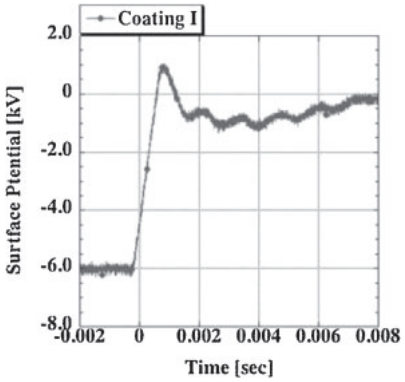

Fig. 11. Assessment test for coating I.

3.3. Validation test

Figure 12 shows solar array coupons in a vacuum chamber under the Type 1 configuration. We compared the charging mitigation performance of solar array coupons with and without a coating. The electron beam irradiation was stopped by closing the shutter and the surface potential distribution was immediately measured on the solar array coupons. Figure 13 shows the surface potential distribution of solar array coupons with and without coating immediately after electron beam irradiation.

Immediately after electron beam irradiation at an energy of 8.5 keV, the potentials of the cover glass and base plate were −300 to −900 V and −1100 V on the coupon without a coating, respectively. Figure 14 shows the surface potential distribution of a solar array coupon without coating 60 min after electron beam irradiation. The surface potential of a solar array coupon without coating was mitigated with an elapsed time, but considerable time was spent to reach a hardly charged-up condition. Since the insulators, which are the cover glass on solar cells and a polyimide film on the base plate, are placed on the coupon surface, there is no conductive path from the cover glass and polyimide film to ground on a coupon. Therefore, surface charging on a coupon cannot be mitigated. In addition to this, the cover glasses have a positive potential with respect to the base plate of the coupon. This state is called an inverted potential gradient on which an electrostatic discharge can easily occur. To prevent on-orbit power system failures in spacecraft due to an electrostatic discharge on solar array panels, we need to mitigate the surface charging, as shown in Fig. 13.

On the other hand, the coupon with a coating was hardly charged up immediately after electron beam irradiation, as shown in Fig. 13. On the coupon with a coating, since Coating H is coated over the entire surface of the coupon, a conductive path is formed from the coupon surface to ground on a coupon. Therefore, the surface charging is mitigated as shown in Figs. 13 and 14. The charging mitigation behavior on the solar array coupons with and without coating is similar to that under all of the electron beam energy conditions. We have confirmed a dramatic improvement of charging

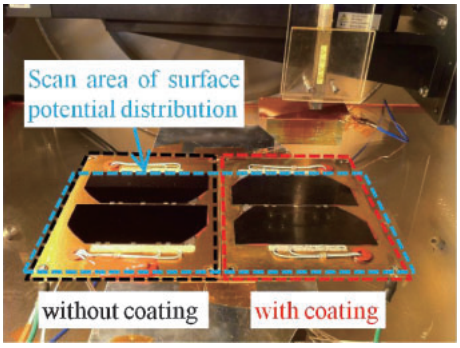

Fig. 12. Solar array coupons on validation test.

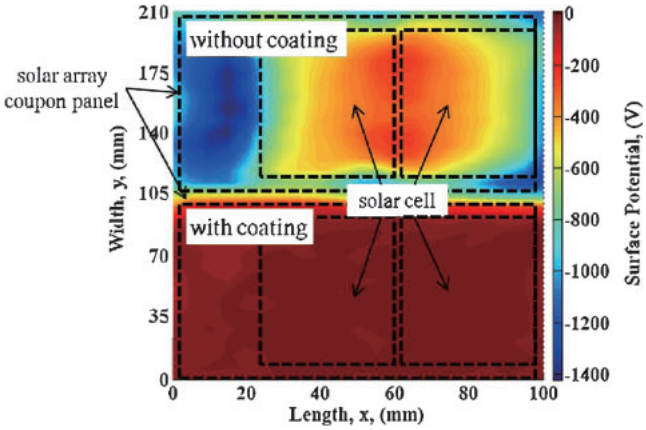

Fig. 13. Surface potential distribution of solar array coupons immediately after electron beam irradiation at the energy of 8.5 keV.

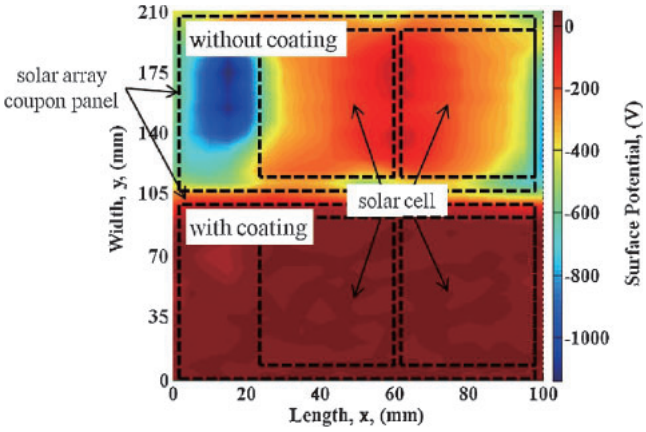

Fig. 14. Surface potential distribution of solar array coupons 60 min after electron beam irradiation.

mitigation by post-coating of a COTS antistatic coating on conventional solar array panels.

4. Future Work

The current developmental goal for antistatic coating is to achieve the following three targets:

1) Electrical power loss due to coating. Due to the coating layer applied on the conventional solar array panel, some solar illumination is obstructed and the generated electrical power leaks through the coating layer. This phenomenon means electrical power is lost on a satellite. From the measurement results of the current-voltage characteristic on solar array coupon panels before and after coating, the electrical power decreased by 21.6% due to the coatings.[6] More efforts are underway to improve this.

2) Space environmental durability. The coating applied on a solar array panel is exposed to harsh space environments, such as the thermal cycle, ultraviolet rays, and charged particle radiations. The charging mitigation performance and optical transparency would degrade in such harsh environments. We must evaluate the environmental durability of the coatings in space.

3) Discharge test for the coated solar array coupon. We must verify that the antistatic coating is effective as a means of preventing discharges on solar array panels. From the experimental results of the discharge test, no discharge arc was observed on solar array coupons with the antistatic coating used in this paper, although discharge arcs were observed on that without coating.[6]

We must continue to improve the anti-static coating agent in the properties of electrical power loss and environmental durability in space, and then we must carry out discharging tests for a solar array coupon panel with an improved coating. We must repeat these processes to reach the optimized coating for space use.

5. Summary

We selected a candidate coating with the required surface resistivity and vacuum resistance. Furthermore, we selected a commercial-off-the-shelf antistatic coating based on conductive nanoparticle dispersed agents, after consideration of the experimental results of charging mitigation performance from simulating charging conditions in space and the degrees of freedom for future coating developments.

The candidate coating agent was applied on a conventional solar array coupon panel and the charging mitigation performance of the coated coupon panel was evaluated. From the experimental results, we have confirmed a dramatic improvement in charging mitigation performance on a coated conventional solar array coupon.

In future work, we hope to improve the electrical power loss due to the coating, evaluate the space environmental durability, and perform a discharging test for a solar array coupon panel with an improved coating. Improvement of the coating agent, evaluation of electrical power loss, space environmental durability tests, and a discharging test to reach the optimized coating will need to be repeated.

Acknowledgments

A part of this work was supported by the Seeds Development Experiment Grant of the Japan Science and Technology Agency.

References

1) Snyder, D. B. and Tyree, E.: The Effect of Plasma on Solar Cell Array Arc Characteristics, NASA TM-86886, 1985.
2) Cho, M.: Arcing on High Voltage Solar Arrays in Low Earth Orbit: Theory and Computer Particle Simulation, Ph.D. Dissertation, Dept. of Aeronautics and Astronautics, Massachusetts Institute of Technology, MA, 1992.
3) Hoeber, C. F., Robertson, E. A., Katz, I., Davis, V. A. and Snyder, D. B.: Solar Array Augmented Electrostatic Discharge on GEO, AIAA Paper 98-1401, 1998.
4) Cho, M. and Nozaki, Y.: Number of Arcs Estimated on Solar Array of a Geostationary Satellite, *J. Spacecraft Rockets*, **42** (2005), pp. 740–748.
5) Dennison, J. R., Swaminathan, P., Jost, R., Brunson, J., Green, N. W., and Frederickson, A. R.: Proposed Modifications to Engineering Design Guidelines Related to Resistivity Measurements and Spacecraft Charging, Proceedings of 9th Spacecraft Charging Technology Conference, CD-ROM, 2005.
6) Takahashi, A., Muraguchi, R., Iwata, M. and Cho, M.: Charging and Arcing Test on Semiconductive Coated Solar Coupon Panel, *IEEE Transactions on Plasma Science*, **42** (2014), pp. 384–390.